

STATIC AND DYNAMIC STRAIN ENERGY RELEASE RATES IN TOUGHENED THERMOSETTING COMPOSITE LAMINATES

Douglas S. Cairns*
Hercules Advanced Materials and Systems Company
(HAMSCO), Magna, UT

22-39
512211
P. 10

Abstract

In this work, the static and dynamic fracture properties of several thermosetting resin based composite laminates are presented. Two classes of materials are explored. These are homogeneous, thermosetting resins and toughened, multi-phase, thermosetting resin systems. Multi-phase resin materials have shown enhancement over homogenous materials with respect to damage resistance. The development of new dynamic tests are presented for composite laminates based on Width Tapered Double Cantilevered Beam (WTDCB) for Mode I fracture and the End Notched Flexure (ENF) specimen. The WTDCB sample was loaded via a low inertia, pneumatic cylinder to produce rapid cross-head displacements. A high rate, piezo-electric load cell and an accelerometer were mounted on the specimen. A digital oscilloscope was used for data acquisition. Typical static and dynamic load versus displacement plots are presented. The ENF specimen was impacted in three point bending with an instrumented impact tower. Fracture initiation and propagation energies under static and dynamic conditions were determined analytically and experimentally. The test results for Mode I fracture are relatively insensitive to strain rate effects for the laminates tested in this study. The test results from Mode II fracture indicate that the toughened systems provide superior fracture initiation and higher resistance to propagation under dynamic conditions. While the static fracture properties of the homogeneous systems may be relatively high, the apparent Mode II dynamic critical strain energy release rate drops significantly. The results indicate that static Mode II fracture testing is inadequate for determining the fracture performance of composite structures subjected to conditions such as low velocity impact. A good correlation between the basic Mode II dynamic fracture properties and the performance in a combined material/structural Compression After Impact (CAI) test is found. These results underscore the importance of examining rate-dependent behavior for determining the longevity of structures manufactured from composite materials.

Introduction

With composite materials being used in primary aerospace structures, some basic understanding of fracture is necessary. This is especially important to develop methodologies for determining damage resistance and damage tolerance of composite structures [1]. "Damage resistance" refers to the ability of a material/structure to sustain an "event" without resulting in damage and "damage tolerance" refers to the ability of a material/structure to maintain performance with damage present. Composite laminates typically have poor, through-the-thickness performance. This makes them especially sensitive to out-of-plane loadings such as bending and impact. The goal is to provide an understanding of fracture such that the performance of laminated structures subjected to low velocity impact can be obtained. For a preliminary assessment of performance, a study of Mode I and Mode II fracture behavior under static and dynamic conditions was conducted. These modes of fracture are important for delamination initiation and propagation for thin, composite laminates subjected to low velocity impact [1-5].

*Research Associate and Manager, Advanced Composites Technology, Magna, UT

Toughened Thermosetting Resin Systems

A relatively new class of thermosetting resin systems for advanced composites is being developed [2-4]. These toughened systems are being developed with better damage resistance and damage tolerance to improve the longevity of aerospace structures such as commercial aircraft. Bradley has noted that an improved process zone in composite laminates is a key for determining interlaminar fracture performance [5]. This process zone is the region between plies and is where interlaminar fracture (delamination) typically occurs. Figure 1a is a photograph of a crack (delamination) in the interply of Hercules IM7/3501-6. Notice that the crack propagates close to the fibers, along one side of the fiber/matrix in a self-similar manner. Some separation of the fracture surface is seen, but the fracture propagates at the ply/matrix interface. This is typical of brittle, homogenous, thermosetting resin systems [6]. Figure 1b is a photograph of an interply crack in Hercules IM7/8551-7. Notice how the interply crack is not self-similar and propagates through and around the different phases. This combination of tough phases and process zone enhancement results in laminates which have superior damage resistance during low velocity impact [7]. Consequently, a basic study to determine the fracture initiation and propagation in this interply region under static and dynamic conditions is necessary for a preliminary understanding of the mechanisms of toughening.

Mode I Test Method

For Mode I fracture performance, the Width Tapered Double Cantilevered Beam Test (WTDCB) was used [8]. A schematic of the geometry used in this study is shown in Figure 2. This sample exhibits a constant fracture load for a given Mode I critical strain energy release (G_{Ic}). From elementary beam theory, for the geometry given in Figure 2, the Mode I critical strain energy release rate, G_{Ic} , is calculated to be:

$$G_{Ic} = \frac{12P^2}{Eh^3} \left(\frac{a}{b} \right)^2$$

If the thicknesses of the halves are unequal;

$$G_{Ic} = \frac{6P^2}{E} \left(\frac{1}{h_1^3} + \frac{1}{h_2^3} \right) \left(\frac{a}{b} \right)^2$$

1)

where h is the half-thickness of the sample and h_1, h_2 are the thicknesses for unequal thicknesses. Hercules uses a nominal specimen which is 152 mm long, 25.4 mm wide, and 3.3 mm thick with a 25 mm precrack. The taper ratio (a/b) is equal to 4.

For static testing, the specimen is simply loaded into a test machine and tested at 2.5 mm/ min. The average load during fracture is recorded and used in Equation 1. A schematic for the Mode I dynamic testing is shown in Figure 3. In this test setup, a low inertia, pneumatic cylinder is used for actuation. The specimen is instrumented with a high-speed, piezo-electric load cell. In addition, an accelerometer is placed on the cross-head to monitor accelerations which are numerically-integrated to determine velocities and displacements. A typical load-time plot is shown in Figure 4. The total fracture time is approximately 9 ms. Notice that, while some deviation in the load is seen during fracture, the load remains relatively constant. Consequently, Equation 1 was used for determining Mode I dynamic critical strain energy release rates (G_{Ic}). Some typical results, comparing static and dynamic Mode I dynamic critical strain energy release rates, are shown in Table 1. Five coupons from each specimen type were used for the tests.

Table 1. Comparison of Static and Dynamic Mode I Fracture Properties

Material Type	Static G_{Ic} J/m ² (in-lbs/in ²)		Dynamic G_{Ic} (Eq.1) J/m ² (in-lbs/in ²)	
IM7/X1	394	(2.25)	312	(1.78)
IM7/X2	256	(1.46)	286	(1.63)
IM7/X4	530	(3.02)	500	(2.85)
IM7/8551-7A	249	(1.42)	202	(1.15)
IM7/8552	233	(1.33)	240	(1.37)
IM7/8551-7	552	(3.15)	607	(3.46)
IM7/8551-7C	381	(2.17)	456	(2.60)

In Table 1, the 8552 is representative of a homogeneous resin system and the X1, X2, X4 and 8551 type resins are representatives of multiphase systems. The coefficient of variation within a panel is typically 5%-6% and the coefficient of variation from panel to panel is typically 10%. With consideration to the variability in this test, the data generally show little sensitivity for the rates tested in this study.

Mode II Test Method

For these basic studies, the End Notched Flexure (ENF) specimen was chosen as a result of its ease to manufacture and test [9-15]. This sample is illustrated in Figure 5. In Figure 5, a beam with a crack in one end is loaded in three point bending to produce interlaminar shear at the midplane. The crack length is denoted as a and the specimen supported length is $2L$ with an overall thickness of $2h$. Under loading, the crack propagates and simple beam theory is used to determine the critical strain energy release rate at fracture. From Linear Elastic Fracture Mechanics (LEFM) and simple beam analysis of the ENF, the Mode II critical strain energy release rate, G_{IIc} may be calculated as [9-11]:

$$G_{IIc} = \frac{9P^2Ca^2}{2w(2L^3 + 3a^3)} \quad 2)$$

where P is the load at fracture, and C is the overall compliance of the specimen. An additional, small correction to account for shearing deformation may be used by replacing C by C^* [11]:

$$C^* = C + \frac{1.2L+0.9a}{4whG_{13}} \quad 3)$$

where G_{13} is the interlaminar shearing stiffness of the specimen. It is noted that, for practical specimen geometries, this correction is less than 2% to the compliance from simple beam theory.

An alternative method for determining the average strain energy release rate during crack propagation may be developed by taking data from the load-displacement curve during testing [16]. In this method, P_i is the load at onset of fracture, and P_a is the load at which the fracture is arrested. By assuming a straight line between P_i and P_a the strain energy release rate may be determined as:

$$G_{IIc} = \frac{P_i\Delta_a - P_a\Delta_i}{2w(a_a - a_i)} \quad 4)$$

where Δ_i, Δ_a are the measured displacements at initiation and arrest, and a_i, a_a are the crack lengths at initiation and arrest. Whitney, et. al. [17] have shown this method to be approximately 10% higher than the compliance method as in Equation 2 for Mode I fracture and Maikuma, et. al. [15] have shown the area method based on energies (which are determined from load versus time data) to be approximately 6% lower for dynamic testing in Mode II fracture. These results are well within the scatter of such fracture tests [11, 17].

To determine the critical strain energy release rates under dynamic conditions, a Dynatup ETI 500 instrumented impact tower was used. A 5.3 kg mass with an impact velocity of 1.93 m/sec was used for the load introduction (kinetic energy equal to 9.8 Joules). The test specimen geometry used for this study was 149.2 mm long (2L) by 25.4 mm wide (w) by 3.3 mm thick (h) with a notch length of 25.4 mm (a). A thin, 0.025 mm Teflon™ film was used for the insert and the crack was propagated to 25.4 mm using Mode I propagation. Fiber bridging was not seen at the crack tip in the composite systems tested in this study. Hercules IM7 fiber was used for most of the studies. This fiber yields an average laminate flexural stiffness of 152 GPa. The average laminate interlaminar shear stiffness is 5.7 GPa.

A typical force versus time and displacement versus time is shown in Figure 6. Knowing the mass of the impactor and the initial velocity, the displacement of the tup is calculated via numerical integration (trapezoidal rule twice) of the directly measured force versus time data. In this figure, the load oscillates up to a peak and drops sharply at the point of fracture. The fracture was rather catastrophic. Under impact, either the sample did not fracture or the crack propagated in an uncontrolled manner in approximately 1 msec with very little change in displacement. Unlike constant crosshead displacement loading conditions, the fracture propagated over the majority of the length of the sample, beneath the loading tup. This is also illustrated in Figure 7 in the load versus displacement plot. While the load oscillates considerably at fracture, the displacement remains relatively constant. Equation 2 (with Equation 3) may be used to predict the initiation strain energy release rate. Note in Figures 6 and 7, a discontinuity in the behavior is seen during fracture. This discontinuity is a result of the flexural wave propagating beneath the load cell. As the crack propagates beneath the impactor, the shape of the curve does not change. That is, if frictional effects are significant as the crack traverses beneath the loading nose, a significant change in the slope in the subsequent behavior would be expected to be seen in the load - displacement curve (Figure 7) as a result of coulomb dissipation. Consequently, frictional effects as the crack propagates beneath the loading tup were assumed to be no more severe than static testing. However, additional studies may be warranted based on some of the unexpected results presented below.

Using Bernoulli-Euler beam theory, the fractured specimen compliance can be determined as:

$$C = \frac{-16L^3 + 36L^2a - 18La^2 + 3a^3}{8Ewh^3} \quad 5)$$

In Equation 5, the crack is assumed to traverse beneath the impactor. This equation is used in a combined analytical-experimental approach to determine the load at crack arrest. By measuring the crack length and using Equation 5, the arrest load is predicted and plotted in Figures 6 and 7, denoted as P_a . This corresponds reasonably well with the average dynamic load at fracture arrest. Consequently, the work of fracture, W , to utilize for average fracture energies during dynamic propagation is:

$$W = \int_0^{\Delta_a} P d\Delta - \frac{P_a}{2} \Delta_a \quad 6)$$

where the integral is the area under the experimental force versus displacement curve and P_a is determined via Equation 5. Some vibratory behavior is present in Figure 6, and Equation 6 represents the average dynamic strain energy release from initiation to arrest. This Equation was used in lieu of Equation 4. In utilizing this equation, it is implied that dynamic effects in the calculation are negligible. This was shown to be true for dynamic tests under similar conditions to the present work by Maikuma, et. al. [15].

Experimental Results

Table 2 is a comparison of Hercules composite systems subjected to static and dynamic Mode II fracture. Five (5) coupons were used for each type of test unless noted. The dynamic fracture behavior presented in Figures 6 and 7 is a combined material and structural test and is dependent on specimen geometry, support conditions, impactor metrics, etc. However, all coupons were tested under the same conditions for consistency.

All laminates are nominally 34% resin content by weight (nominally 58.8% fiber volume). The X8553, 8551-7 and X series laminates are multi-phase, process zone enhanced laminates similar to Figure 1b; while the 3501-6 and 8552 resin type laminates are homogeneous with limited process zones in the interply region, similar to Figure 1a [4,5]. The process zone enhanced laminates exhibit higher Mode II toughnesses than the homogeneous systems. The X2 resin is a toughened system formulated to have superior hygrothermal properties (hot/wet 0° compression performance) but exhibits lower Mode II toughness than other systems. Two resin contents were tested in the X2 formulation as noted. The higher resin content X2 system exhibits higher Mode II fracture properties.

In Table 2, there is not necessarily a correlation between static Mode II and dynamic Mode II fracture properties. This is especially evident in the case of the homogeneous systems. While the 8552 exhibits the poorest static Mode II interlaminar fracture toughness, it has better Mode II dynamic properties. Its damage resistance in low velocity impact is superior as well [18]. The AS4/3501-6 exhibits the poorest damage resistance in low velocity impact. Notice that it also has the lowest initial dynamic strain energy release rate as defined by Equation 2 (with the minor shearing correction suggested in Equation 3). Upon initiation, the average fracture resistance as determined by Equations 4 and 6 drops dramatically compared to the other materials. The Average Dynamic G_{IIc} (Eq. 6) of the AS4/3501-6 is less than half of the Dynamic G_{IIc} (Eqs. 2,3) and considerably lower than the static Mode II fracture properties. Once fracture initiates, the resistance to propagation is lower in the AS4/3501-6 system, resulting in more damage (delamination) under dynamic conditions [2]. Similar trends have been noted by other investigators [13,15] for the same 3501-6 resin system. The homogeneous resin laminates appear to be much more strain rate sensitive than the toughened systems. Hence, static fracture properties may not be applicable for determining the damage resistance, damage tolerance and longevity under dynamic conditions.

Table 2. Comparison of Static and Dynamic Mode II Fracture Properties

Material Type	Static G_{IIc} J/m ² (in-lbs/in ²) [CV ¹]			Dynamic G_{IIc} (Eq. 2) J/m ² (in-lbs/in ²) [CV ¹]			Average Dynamic G_{IIc} (Eq. 6) J/m ² (in-lbs/in ²) [CV ¹]		
IM7/8551-7	1867	(10.6)	[5.6]	2730	(15.5)	[3.9]	2272	(12.9)	[8.3]
IM9/8551-7	1691	(9.6)	[7.5]	2184	(12.4)	[7.2]	1832	(10.4)	[10.5]
IM7/X8551-7C	1374	(7.8)	[2.6]	2360	(13.4)	NA ⁴	1744	(10.2)	[12.7]
IM7/X1	1268	(7.2)	[5.9]	2202	(12.5)	[4.7]	2184	(12.4)	[3.5]
IM7/X2 ²	1426	(8.1)	[3.5]	1726	(9.8)	[3.5]	1920	(10.9)	[2.4]
IM7/X2 ³	1268	(7.2)	[5.9]	1691	(9.6)	[8.4]	1761	(10.0)	[6.3]
IM7/X3	1374	(7.8)	[7.8]	1814	(10.3)	[19.7]	1462	(8.3)	[27.1]
IM7/X4	1532	(8.7)	[5.6]	2078	(11.8)	[6.9]	2078	(11.8)	[4.3]
AS4/3501-6	740	(4.2)	[7.1]	916	(5.2)	[5.3]	463	(2.6)	[7.0]
AS6/8552	617	(3.5)	[6.1]	1532	(8.7)	NA ⁴	1391	(7.9)	NA ⁴

¹CV (Coefficient of Variation, % based on five (5) replicates for each test

²IM7/X2 at 39% resin content (by weight)

³IM7/X2 at 32% resin content (by weight)

⁴ average of two samples

Compression After Impact

Compression After Impact (CAI) testing is often used for early screening assessment of performance of materials [2-4,7,18,19]. In this test, a quasi-isotropic panel (102 mm x 152 mm X 4.5 mm) thick is impacted with 667 N-m/m(thickness) impact energy at low velocity (approximately 2.5 m/s) with a 12.7 mm diameter tup. This test is a combined damage resistance and damage tolerance test wherein damage is introduced during the impact event and subsequently tested in an end loaded compression fixture with semi-clamped

ends. A schematic of the CAI test setup is shown in Figure 8. A plot of CAI performance versus the Average Dynamic G_{IIc} presented in Table 2 is shown in Figure 9. The high and low data points are shown with error bars.

The CAI test is primarily a damage resistance test. The materials given in Table 1 have similar static damage tolerance performance based on open hole compression (OHC) tests and compression tests of laminates with similar impact damage [18]. That is, given an equivalent, pre-existing damage state, the materials deliver the same static strength. The average OHC performances for the X8553, 8551-7, X-Series, 3501-6, and 8552 based laminates are 300 MPa, 293 MPa, 287 MPa, 300 MPa, and 320 MPa, respectively. However, the materials in Table 2 exhibit dramatically different damage resistance performance under dynamic conditions such as low velocity impact. Specifically, the static G_{IIc} data presented in Table 2 for the 3501-6 based laminate is higher than the 8552 laminate, but this situation is reversed under dynamic conditions. Thus, the Average Dynamic G_{IIc} appears to be a leading indicator for a preliminary assessment of the advanced composite laminates subjected to lateral impact. It is a measurement of the average strain energy release rate for Mode II fracture during delamination formation under dynamic loading conditions.

Conclusions and Recommendations

In this study, an assessment of Mode I and Mode II fracture under static and dynamic conditions has been developed. Rate had little effect for the rates and materials tested in Mode I in this study. The rates tested are typical of the impact duration of low velocity impact [1]. Higher testing rates may show a stronger effect. In contrast, the Mode II fracture performance of toughened systems is considerably better than homogeneous, brittle systems. While the apparent dynamic fracture properties of the systems are higher under dynamic conditions, the fracture performance of the toughened multi-phase systems appears to be less strain rate sensitive than the homogeneous systems. These results establish the need to examine dynamic fracture properties of materials for assessment of damage resistance during low velocity impact.

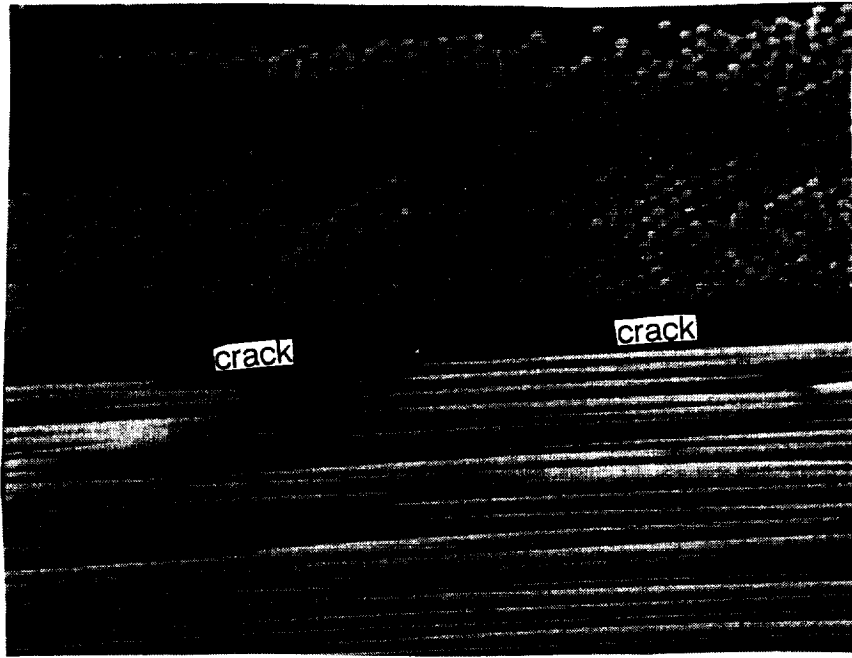
The simple, dynamic Mode II fracture test presented herein is somewhat easier to run, and considerably less expensive than CAI testing. Also, it has more meaning since it provides a measurement of a basic fracture mode, rather than a combined damage resistance, damage tolerance and structural test. The strong trend presented in Figure 9 should not be taken as a panacea, as the ultimate goal of increased longevity of composite materials is a combined damage resistance and damage tolerance problem. A combination of tests under static and dynamic conditions is necessary to determine the longevity of a material and structure.

Future tests should include a wider variety of materials, including thermoplastics, which are known to be quite strain rate sensitive [5]. In addition, a study varying the specimen geometry, loading conditions and impactor metrics should be conducted to isolate the influence of structural and material parameters of fracture performance.

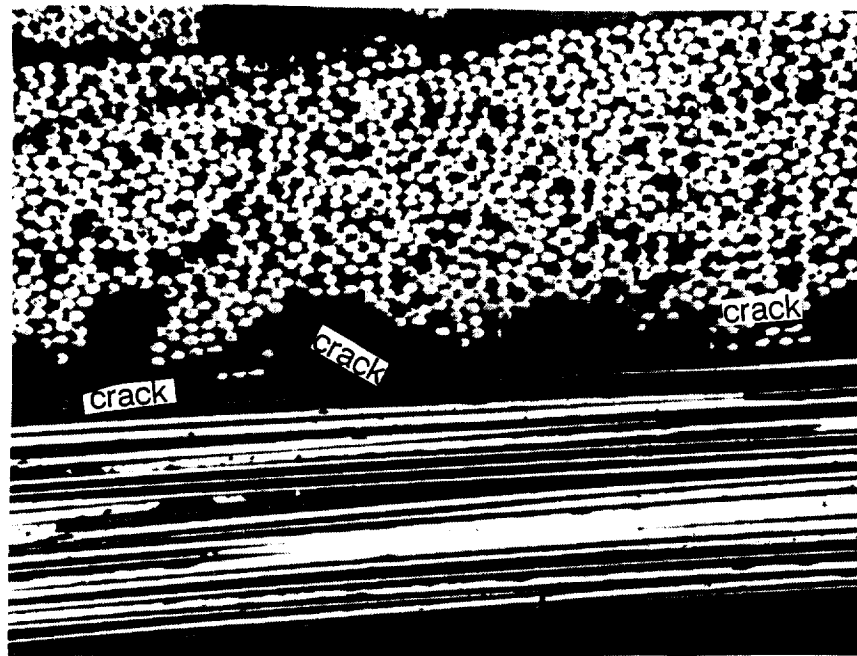
REFERENCES

1. Cairns, D.S. and Lagace, P.A., "A Consistent Engineering Design Methodology for Composite Structures Subjected to Impact", **Proceedings of the American Society for Composites: Fifth Technical Conference**, June, 1990.
2. Boll, D.J., Bascom, W.D., Weidner, J.C. and Murri, W.J., "A Microscopy Study of Impact Damage of Epoxy-Matrix Carbon-Fiber Composites," **Journal of Materials Science**, Volume 21, 1986.
3. Cairns, Douglas S., "Prediction of Fracture Toughness of Multi-Phase Materials", **Proceedings of the AIAA/ASME/ASCE/AHS/ASC 31st Structures, Structural Dynamics and Materials Conference**, April, 1990.
4. Cairns, D.S., "Mechanisms of Fracture and Toughening in Multi-Phase Materials", **Proceedings of the 22nd International SAMPE Technical Conference**, Volume 22, November 6-8, 1990.

5. Bradley, W.L., "The Role of Matrix Properties on the Toughness of Thermoplastic Composites," Prepared for **Thermoplastic Composite Materials**, Series Editor - R. Byron Pipes, Volume Editor - Leif A. Carlsson, Elsevier Science Publishers, 1989.
6. Lagace, P.A. , "Static Tensile Fracture of Graphite/Epoxy," TELAC Report 182-4, Massachusetts Institute of Technology, Cambridge, Massachusetts, 1982.
7. Dost, E.F., Ilcewicz, L.B., and Gosse, J.H., "Sublaminar Stability Based Modeling of Impact-Damaged Composite Laminates," **Proceedings of the American Society for Composites: Third Technical Conference**, September, 1988.
8. Bascom, W.D. and Hunston, D.L., "The Fracture of Epoxy and Elastomer-Modified Epoxy Polymers," **Treatise on Adhesion and Adhesives, Volume 6**, Edited by Patrick, Robert L., Marcel Dekker, Inc., New York, 1989.
9. Russell, A.J. and Street, K.N., "Moisture and Temperature Effects on the Mixed-Mode Delamination Fracture of Unidirectional Graphite/Epoxy, **Delamination and Debonding of Materials**, ASTM STP 876 (1985), American Society for Testing and Materials, Philadelphia, PA, p. 349.
10. Carlsson, L.A. and Pipes, R.B., **Experimental Characterization of Advanced Composite Materials**, Prentice-Hall, Englewood Cliffs, New Jersey, 1987.
11. Carlsson, L.A. and Gillespie, J.W., Jr., "On the Design and Analysis of the End Notched Flexure (ENF) Specimen for Mode II Testing," **Journal of Composite Materials**, vol. 20, 1986.
12. Smiley, A.J. and Pipes, R.B., "Rate Effects on Mode I Interlaminar Fracture Toughness in Composite Materials," **Journal of Composite Materials**, vol. 21, 1987, pp. 671-687.
13. Smiley, A.J. and Pipes, R.B., "Rate Sensitivity of Mode II Interlaminar Fracture Toughness in Graphite/Epoxy and Graphite/PEEK Composite Materials," **Composites Science and Technology**, vol. 29, 1987, pp. 1-15.
14. Friedrich, K., Walter, R., Carlsson, L.A., Smiley, A.J., and Gillespie, J.W., Jr., "Mechanisms for rate effects on interlaminar fracture toughness of carbon/epoxy and carbon/PEEK composites," **Journal of Materials Science**, vol. 24, 1989, pp. 3387-3398.
15. Maikuma, H., Gillespie, J.W., Jr., and Wilkins, D.J., "Mode II Interlaminar Fracture of the Center Notch Flexural Specimen under Impact Loading," **Journal of Composite Materials**, vol. 24, 1990, pp. 125-149.
16. Wu, E.M., "Fracture Mechanics of Anisotropic Plates," in **Composite Materials Workshop**, Tsai, S.W., Halpin, J.C. and Pagano, N.J., editors, Technomic Publishing Co., Westport, CT, 1968, pp. 20-43.
17. Whitney, J.M., Browning, C.E. and Hoogsteden, W. "A Double Cantilever Beam Test for Characterizing Mode I Delamination of Composites," **Journal of Reinforced Plastics and Composites**, vol. 1, 1982, p. 297.
18. **Hercules Prepreg Tape Materials Characterization Data Package**, Fibers: AS4, IM6, IM7 & IM8, Resins: 8551-7, 8551-7A, 8552, 3501-6, Hercules Composite Products Group, Magna, Utah, November, 1988.
19. Dost, E.F., Ilcewicz, Avery, W.B., and Coxan, B.R., "The Effects of Stacking Sequence on Impact Damage Resistance and Residual Strength for Quasi-Isotropic Laminates," **Proceedings of the American Society for Composites: Fifth Technical Conference**, June, 1990.



a) AS4/3501-6 (self-similar crack at ply/matrix interface)



b) IM7/8551-7 (non self-similar, tortuous crack in interply process zone)

Figure 1. Crack Propagation in Hercules a) AS4/3501-6 and b) IM7/8551-7

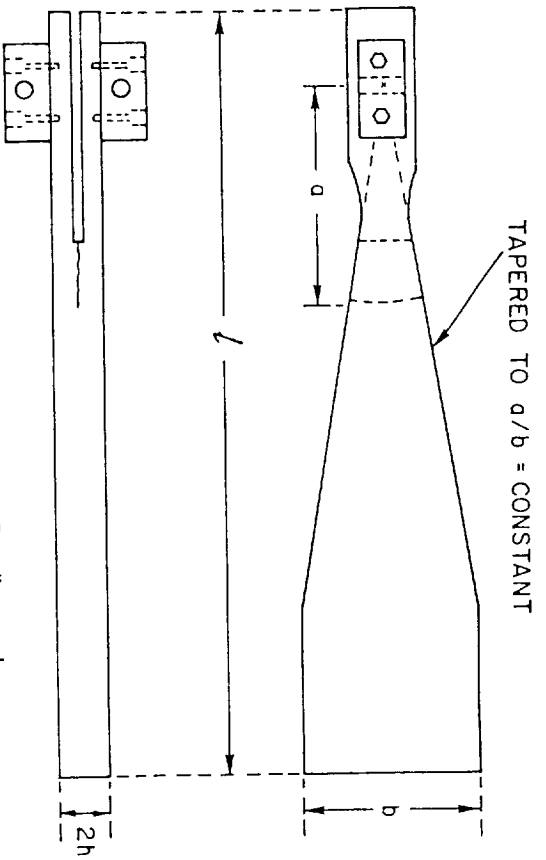


Figure 2. Width Tapered Double Cantilevered Beam (WTD CB) Geometry

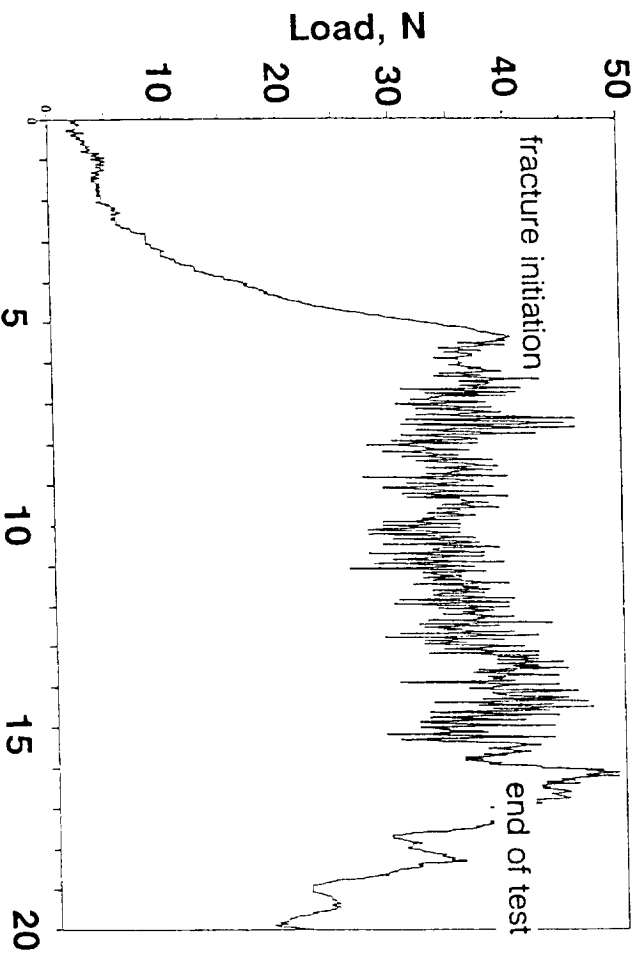


Figure 4. Load versus Time for Dynamic Mode I Fracture Testing

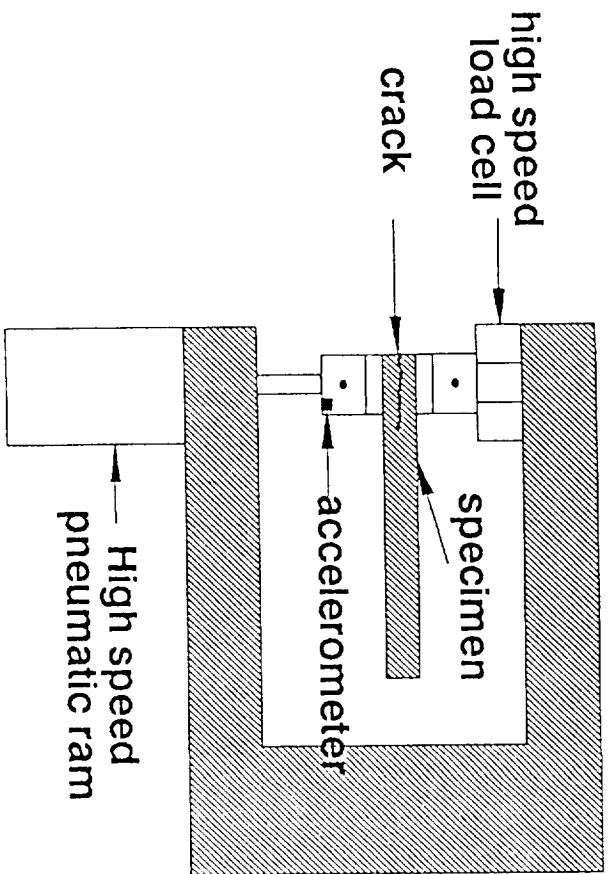


Figure 3. Test Setup for Dynamic G_c Testing

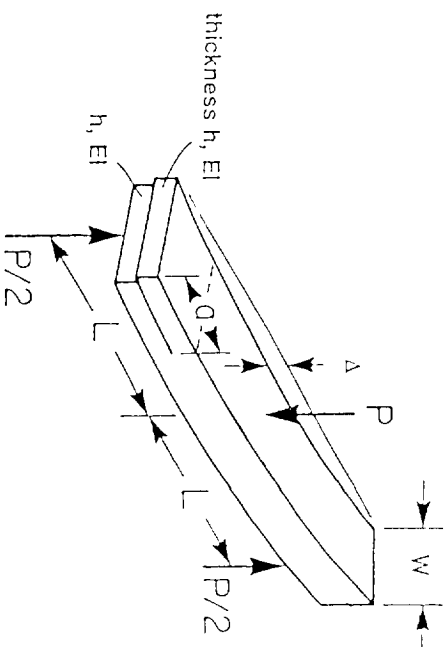


Figure 5. End Notched Flexure (ENF) Geometry

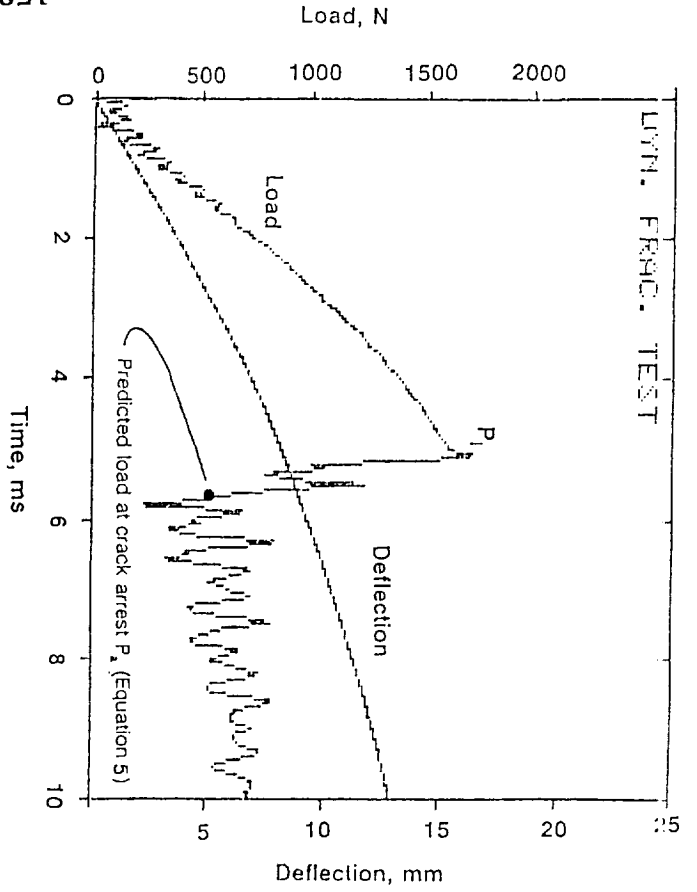


Figure 6. Load versus Time for Dynamic Mode II Fracture Testing

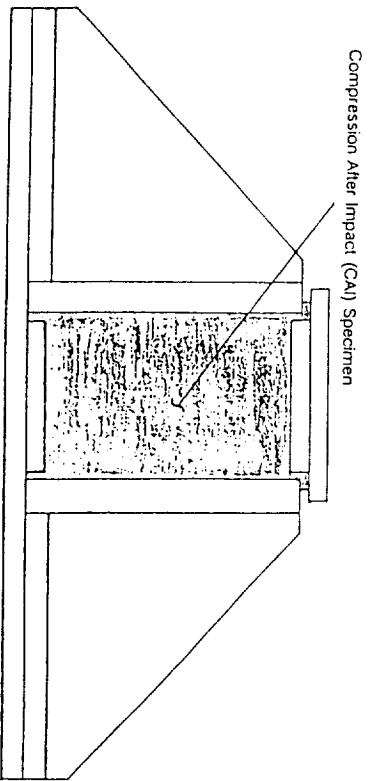


Figure 8. Schematic of Compression After Impact (CAI) Test Setup

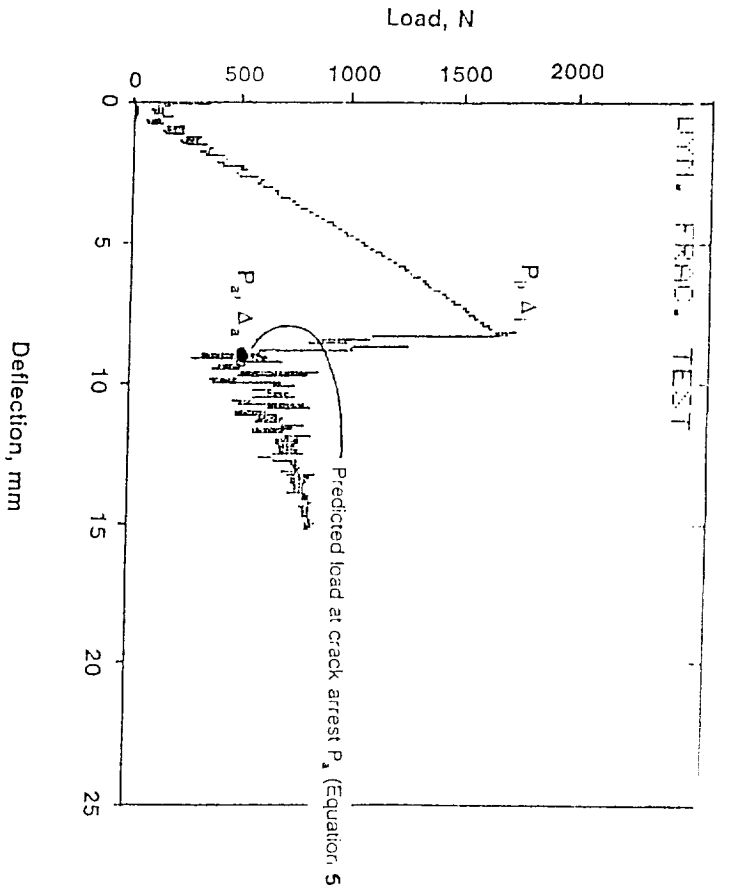


Figure 7. Load versus Deflection for Dynamic Mode II Fracture Testing

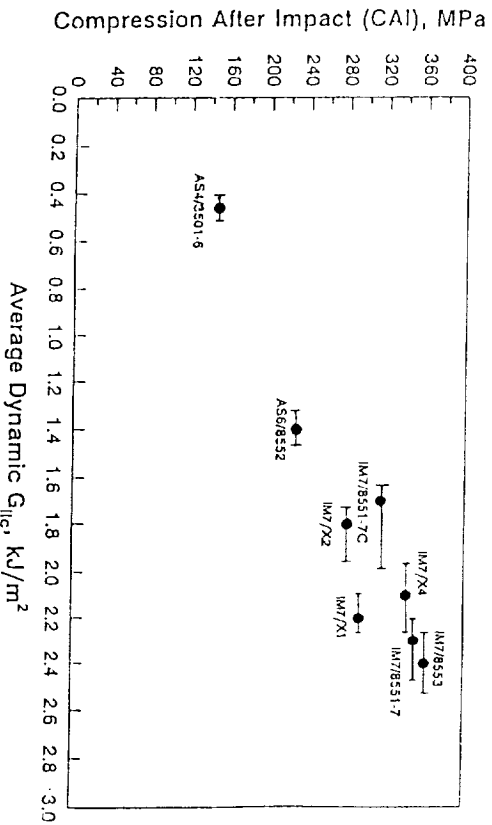


Figure 9. Compression After Impact Performance versus Average Dynamic G_{IIc}